Journal of Applied Polymer Science

Microstructure Evolution of SW/EPN Composites During Hot Air Aging

Hong-Mei Xiao,[1] Mao-Sheng Zhan,[2] Wen Xu,[2] Xiao-jun Ding[2]

[1]Key Laboratory of Aerospace Materials and Performance (Ministry of Education), School of Materials Science and Engineering, Beihang University, Beijing 100191, China

[2]Aerospace Research Institute of Materials and Processing Technology, Beijing 100076, China

Correspondence to: M.-S. Zhan (E-mail: zhanms@buaa.edu.cn)

ABSTRACT: In this article, the hot air aging of high strength glass fiber fabric/epoxy novolac resin (SW/EPN) composites was investigated by the aid of the aging behavior of EPN, mainly focusing on the microstructure evolvement of SW/EPN composites. The aging mechanism and thermal mechanical properties of SW/EPN composites were analyzed by Fourier transform infrared spectroscopy, X-ray photoelectron spectroscopy, thermo-gravimetric analyzer coupled with Fourier transform infrared spectrometry, and dynamic mechanical thermal analysis. The results showed that micro cracks initiated and propagated at the fiber–matrix interphase because of the heat and oxygen effect. After long-time aging at elevated temperatures, delamination phenomenon was discovered in SW/EPN composites. The results of weight changes showed that the degradation of EPN played a major role in SW/EPN composites. Moreover, the degradation of EPN contained post-curing, oxidation, and decomposition. The results also revealed that unaged EPN indicated two glass transition temperatures (T_{g1} and T_{g2}). T_{g1} increased for post curing while T_{g2} decreased for oxidation with increasing of aging time and temperature. In the final period of aging at higher temperatures, only one T_g was observed because the formation of perfect crosslinked networks made EPN homogeneous. In addition, the relationship between T_g and chemical structure, as well as T_g and mass loss, confirmed that the variation of T_g depended on chemical changes. © 2013 Wiley Periodicals, Inc. J. Appl. Polym. Sci. **2014**, *131*, 40128.

KEYWORDS: ageing; degradation; composites; structure–property relations; properties and characterization

Received 9 September 2013; accepted 27 October 2013

DOI: 10.1002/app.40128

INTRODUCTION

Advanced fiber reinforce polymer composites easily degrade in the service or storage period due to the effects of the season temperature and the oxygen in air.[1,2] Previous researches have shown that epoxies and related composites degrade when exposed to temperatures 150°C.[3,4] The degradations involving physical and chemical changes lead to discoloration, structural damage, and the deterioration of mechanical and thermal properties. However, for the different epoxy resin reinforced composites, the aging behavior is not exactly the same. Therefore, it is necessary to study the microstructure evolution and the aging mechanism of epoxies and related composites in order to evaluate the service reliability.

The interface evolvement, the matrix degradation, and the mechanical degradation of epoxy composites under hot air condition have been studied in many papers, mainly focusing on the behavior of neat resins and carbon fiber/epoxy composites at the microscopic scale. The interface evolvement of carbon fiber/epoxy composites have been investigated by Lafarie-Frenot and coworkers.[5–7] They found that oxidative thermal degradation induces matrix shrinkage which generates thermal-mechanical stress, leading to cracks initiation and propagation.[5,6] Moreover, the shrinkage is not only related to aging condition, including aging time, aging temperature, and oxygen pressure, but also connected with the distance between fibers.[7] For the matrix degradation, many studies suggest that the chemical reaction during thermal-oxidative aging consists of post cure,[4,8] oxidation,[9,10] and chain scission.[11,12] According to Celina et al., epoxy resin is reactive between 25 and 140°C, and the oxidation sensitivity obeys an excellent Arrhenius behavior with activation energies in the 70–80 kJ/mol range.[3] The oxidation of neat resin is limited to superficial layers owing to its kinetic control by O_2 diffusion.[13] However, the composites microstructure, the fiber/matrix interphase, and damage mechanisms introduce anisotropy in the diffusion and oxidation behavior, and the anisotropic oxidation of the composites is analyzed by Fourier transform infrared spectroscopy (FTIR)[13] and scanning electron microscope (SEM).[14] These researches also reveal that the post cure, oxidation, and decomposition of matrix are the main degradation mode.

The degradation of materials can be monitored by the glass transition temperature (T_g). Numerous studies have shown that the

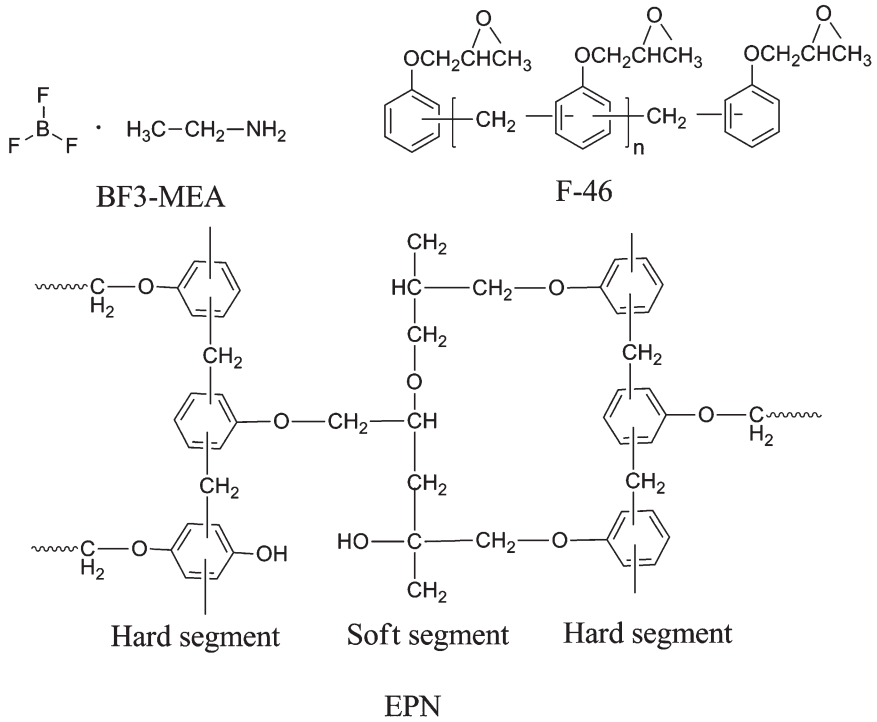

Figure 1. Chemical structures of the BF_3-MEA, F-46, and EPN.

variation of the T_g more or less depends on the aging temperature. The T_g of the glass-mica-epoxy insulations aged at 130°C rises with time because of the increasing crosslinking of the epoxy.[15] However, the T_g initially increases and then decreases after aging at 155°C,[16] 180°C,[15] or 210°C,[17] there are two possible explanations for the decrease of T_g, including the plasticization of the matrix[16] and the degrading of the material.[17] For the DGEBA/EPN/LMPA epoxy system (hereinafter referred to as diglycidyl ether ofbisphenol-A and novolac epoxy resin blends cured with low molecular polyamide) investigated by Pei et al., there are two T_g due to the formation of "skin-core" structure during thermal-oxidative aging.[4] Overall, the relationship between T_g and chemical changes during aging has rarely been investigated.

Up to now, numerous studies have been performed to investigate the aging behavior of carbon fiber/epoxy composites during hot air aging. However, the thermal air aging behavior of glass fiber/epoxy composites has rarely been studied. In this study, high strength glass fiber fabric/epoxy novolac resin (SW/EPN) composites were selected as the research object. The microstructure changes of SW/EPN composites during hot air aging were investigated by SEM, FTIR, X-ray photoelectron spectroscopy (XPS), thermogravimetric analyzer coupled with Fourier transform infrared (TGA-FTIR) spectrometry, and dynamic mechanical thermal analysis (DMTA). In addition, the relationship between T_g and chemical structure, as well as T_g and mass loss, was discussed. These works provide insightful evidence to understand the aging behavior of SW/EPN composites in service and storage period.

EXPERIMENTAL

Samples and Aging Condition

The neat EPN samples were prepared by molten casting molding with the epoxy resin (F-46) with the structure of phenol and epoxy.[18] Meanwhile, boron trifluoride ethylamine (BF_3.MEA) was selected as curing agent, and the mass ratio of epoxy resin F-46 and BF_3.MEA is 100 : 3. Epoxy resin F-46 was purchased from Shanghai Resin Factory, and BF_3.MEA was supplied by Shanghai SSS Reagent Co. The chemical structures of the F-46, BF_3.MEA, and EPN are detailed in Figure 1.

The SW/EPN composite laminates were manufactured with dried prepregs by hand lay-up and autoclave molding. The material was supplied by Aerospace Research Institute of Materials and Processing Technology, containing about 70% of fibers. The SW/EPN composite laminates were composed of satin-woven glass fabric (SW-180D-90A), supplied by Nanjing Fiberglass Research and Design Institute, and epoxy resin F-46. The structural diagram of SW/EPN composite laminates is shown in Figure 2.

Five specimens were prepared for each testing according to test requirement. The hot air aging was carried out in ventilated ovens, ESPEC facilities (Japan) H201. The aging temperatures were set at 110°C, 130°C, 150°C, and 170°C, respectively. The aging time was up to 90 days.

Characterization Methods

Characterization of Physical Change. The surface color was recorded by SONY DSC-WX300 digital camera. The mass loss was measured by Sartorius BS-124S electronic balance, and the mass of original samples was 4 ± 0.2 g and the dimension of samples is $30 \times 8 \times 4$ mm^3. The surface morphology was observed by Camscan Apollo 300 field emission scanning electron microscope (FE-SEM). Thermal degradation was analyzed with a TGA-FTIR system, which consisted of a Netzsch STA 449F3 instrument coupled to an Bruker VERTEX 70 FTIR system. IR spectra were recorded in the spectral range 4000–500

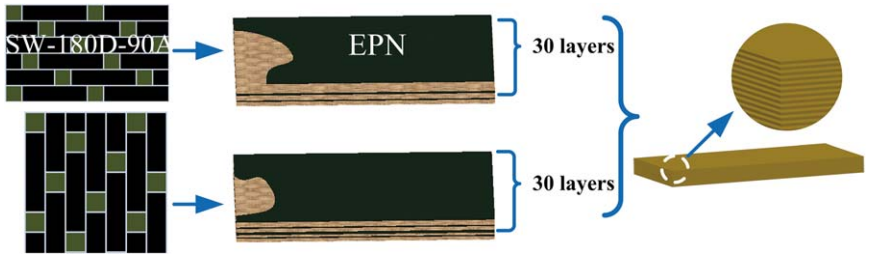

Figure 2. Structural diagram of SW/EPN composite laminates. [Color figure can be viewed in the online issue, which is available at wileyonlinelibrary.com.]

cm^{-1} with a resolution of 8 cm^{-1}. Specimens were heated from 30 to 800°C at a rate of 10°C/min in Argon gas atmosphere. Epoxy resin is reactive and can be oxidized in the oxygen atmosphere.[3] In order to study the decomposition of materials without influence of oxygen, Argon gas atmosphere was selected in this study.

Characterization of Chemical Structure. The specimens before and after thermal air aging were analyzed by FTIR spectroscopy with a Nixolet Nexus-470 spectrometer. The spectra were recorded at a resolution of 4 cm^{-1} between 4000 cm^{-1} and 500 cm^{-1}. XPS measurements were performed using an ESCALAB 250 spectrometer, equipped with a monochromatic X-ray source (Al Kα) operating at 200 W. A spot of 650 μm in diameter, 200 eV of pass energy for survey scan, and 30 eV for high resolution scan were used in all the measurements. The software XPSPEAK4 was used to fit the XPS spectra peaks, and a five-parameter curve fitting was conducted for the C_{1s} spectra by taking 284.8 eV as the reference peak.

Characterization of Thermal-Mechanical Property. Thermal-mechanical tests were carried out with a DMA Q800 analyzer. The geometry of deformation was the three-point blending mode. These tests were performed in the scanning temperature mode, in a range from 25 to 280°C at a heating rate of 5°C/min, and with an oscillating frequency of 1.0 Hz. The dimensions of the specimens were 30 × 4 × 2 mm^3.

RESULTS AND DISCUSSION

Physical Changes of SW/EPN Composites

Surface Colors of SW/EPN Composites. As shown in Figure 3, for the SW/EPN composites that aged in hot air, the following color changes are observed: initially light yellow to yellow-brown, with a gradual shift from yellow-brown to brown-red, and finally to black. The higher the aging temperature is, the shorter the required time of turning black is. After aging for 90 days, all the specimens turn into black. The color changes are indicative of the formation of chromophore groups, such as carbonyl and quinone. These phenomena demonstrate that chemical changes occur in composites due to thermo-oxidative degradation.

Weight Loss of SW/EPN Composites. The weight of SW/EPN composites during thermal air aging is shown in Figure 4. It can be observed that the weight decreases rapidly during the initial aging period because of the loss of moisture and the volatilization of small molecular compounds. Moreover, the higher the aging temperature is, the larger the weight change ratio is. In the final aging period, the trends of weight changes are different for different aging temperatures. Above 150°C, the mass decreases significantly because of the thermal oxidative decomposition. However, the mass increases slightly when aged at 110°C or 130°C. The increased mass may be attributed to uncertainty in measurement. After aging for 90 days at 110°C, 130°C, 150°C, and 170°C, the mass loss ratio reaches 0.13%, 0.43%, 1.08%, and 3.12%, respectively.

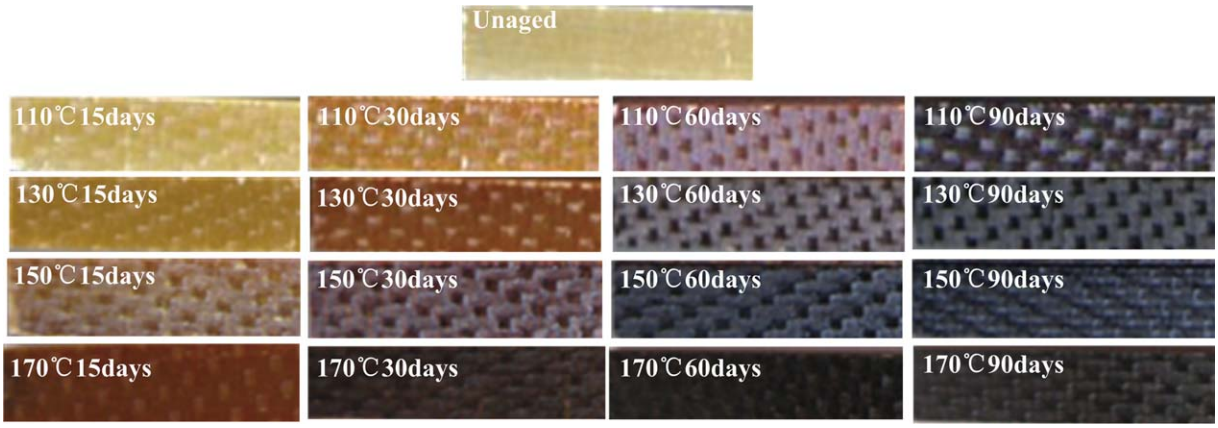

Figure 3. Digital photos of SW/EPN composites specimens during hot air aging. [Color figure can be viewed in the online issue, which is available at wileyonlinelibrary.com.]

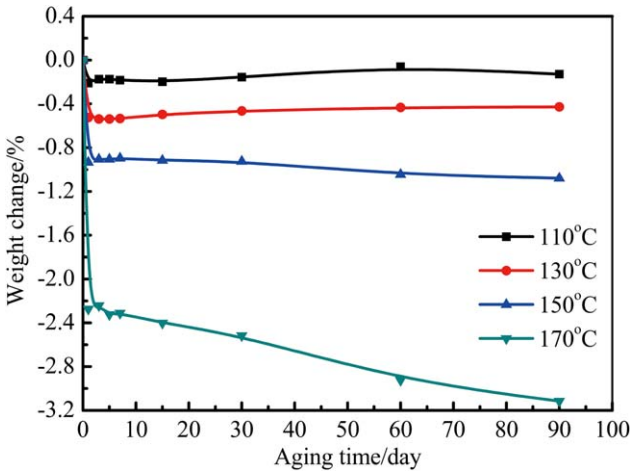

Figure 4. Weight changes of SW/EPN composites specimens during hot air aging. [Color figure can be viewed in the online issue, which is available at wileyonlinelibrary.com.]

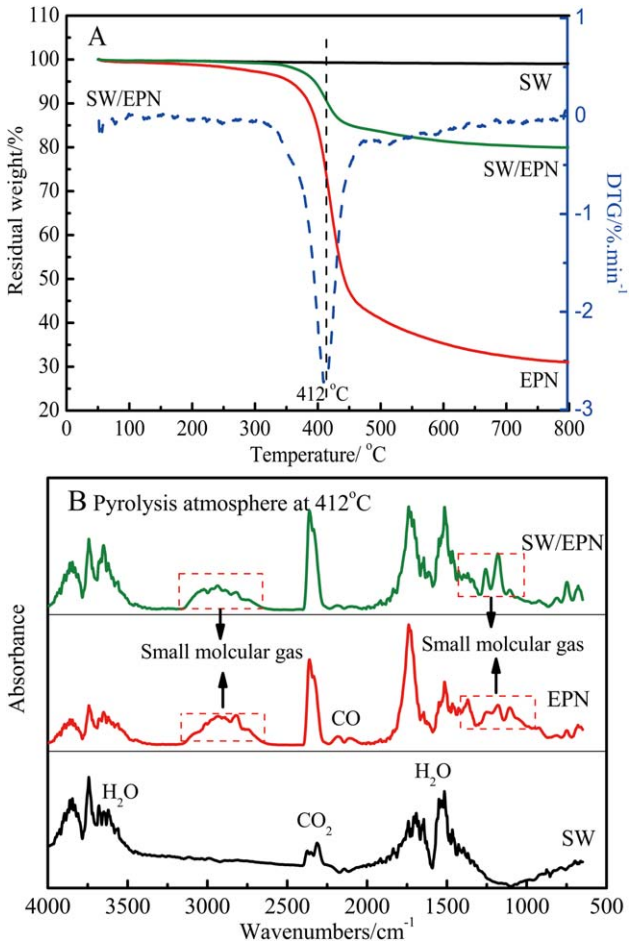

Figure 5. TGA-FTIR curves for SW, EPN, and SW/EPN composites. A: TGA curves for SW, EPN, and SW/EPN composites and the corresponding DTG curves for SW/EPN composites. B: FTIR spectra for the decomposition products of SW, EPN, and SW/EPN composites at 412°C. [Color figure can be viewed in the online issue, which is available at wileyonlinelibrary.com.]

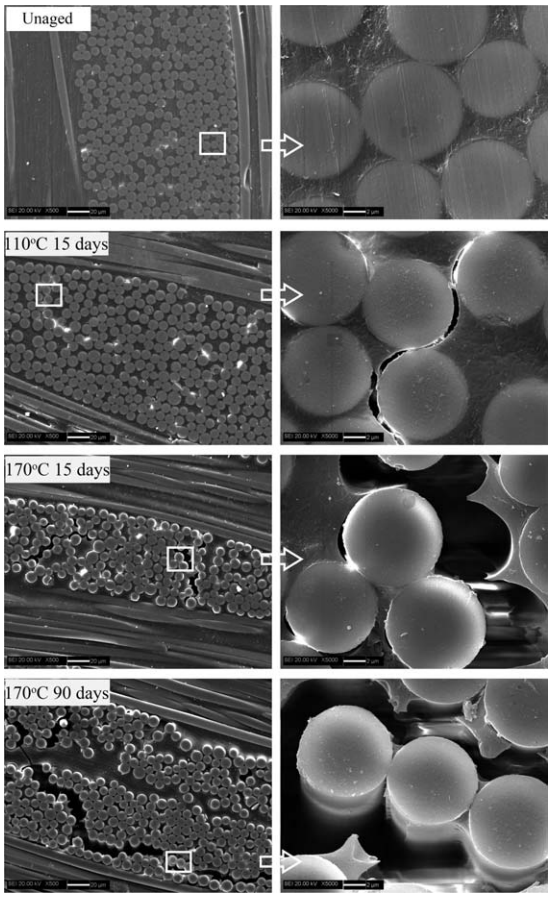

Figure 6. SEM micrographs of the polished cross-section of SW/EPN composites after hot air aging.

In order to determine the contribution of the components of SW/EPN composites, the mass losses versus temperature of SW, EPN, and SW/EPN composites were studied by TGA-FTIR. The thermal degradation behavior of SW, EPN, and SW/EPN composites is shown in Figure 5(A). The graph indicates that the main mass loss of EPN and SW/EPN occurs at the temperature range from 320 to 480°C. The weight of SW drops slightly while the weight of EPN declined dramatically. The final mass ratios of SW, EPN, and SW/EPN composites at 800°C are 99.06%, 31.06%, and 79.96%, respectively. In addition, the results in Figure 5(B) show that the volatile degradation products of SW are H_2O and a small amount of CO_2. The degradation products may derive from the impurities on the glass fibers and the moisture due to insufficient drying of the glass fibers. Besides H_2O and CO_2, the pyrolysis products of EPN and SW/EPN composites contain CO and other small molecular gas. It can be concluded that the degradation of SW/EPN composites is mainly assigned to the degradation of EPN.

Interface Evolution of SW/EPN Composites. Figure 6 shows SEM micrographs of polished edge of SW/EPN composites after hot air aging. No surface fiber–matrix debonding is visible in unaged specimen. After aging for 15 days at 110°C, the debonding damage occurs at the fiber–matrix interphase in the form of

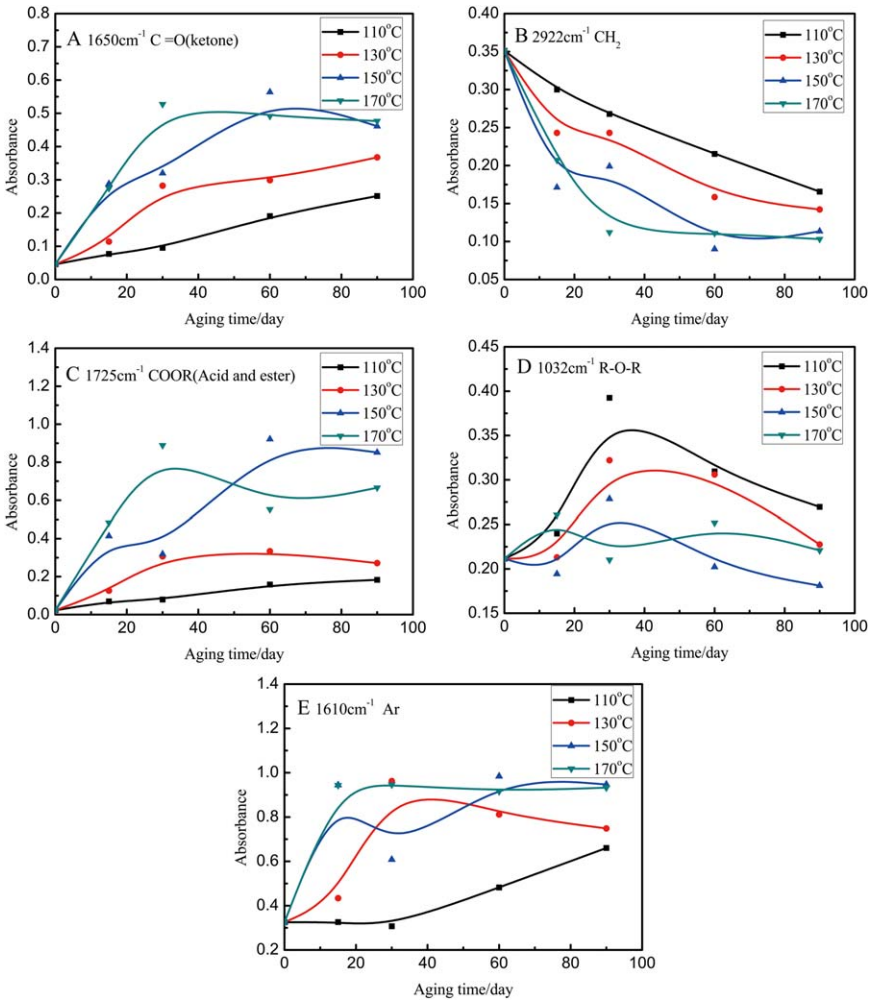

Figure 7. Absorbance of main characteristic bands of EPN during hot air aging (A) 1650 cm^{-1}, C═O (B) 2922 cm^{-1}, CH_2 (C) 1725 cm^{-1}, COOR (D) 1032 cm^{-1}, R—O—R (E) 1610 cm^{-1}, Ar. [Color figure can be viewed in the online issue, which is available at wileyonlinelibrary.com.]

interface debonding and cracks, indicating interfacial bond weaken. Furthermore, as aging time and temperature increase, cracks expand gradually and then connect together accompanied by the matrix shrinkage. The matrix shrinkage is related to the volatilization of small molecules produced during post curing and pyrolysis products generated during thermal decomposition. It can be confirmed that cracks are caused by matrix shrinkage which generates local stress.[5] Delamination phenomena are evident for the specimen aged at 170°C for 90 days. However, SW and neat matrix display no defects during the overall aging process. These results illustrate that interface is the weakest part in SW/EPN composites. Furthermore, the interfacial damage may have a direct relationship with thermal oxidation of EPN.

Chemical Changes of EPN

When exposed to hot air conditions, EPN degrades and leads to the variation of chemical structure. The intensity changes of main characteristic bands of EPN during hot air aging are shown in Figure 7, including the bands at 1650 cm^{-1} (carbonyl, C═O), 2922 cm^{-1} (methylene, CH_2), 1725 cm^{-1} (acid or ester, COOR), 1610 cm^{-1} (benzene ring, Ar), and 1032 cm^{-1} (Ether, R—O—R).

Methylene in EPN may be oxidized to carbonyl after thermal air aging.[4,19] Here, the band near 1650 cm^{-1} refers to the C═O in diphenylketone and quinone. As aging time elapses, the band of C═O rises with the decline of the CH_2 as shown in Figure 7(A,B). Moreover, the uptrend of C═O coincides with the downward trend of CH_2. This means that the CH_2 between two benzene rings is oxidized to diphenylketone.[4,20] The higher the aging temperature is, the faster the oxidation rate is. The absorption band of C═O begins to decline slightly at 150°C aging for 60 days or 170°C aging for 30 days, suggesting that the generated diphenylketone is decomposed. The phenomenon implies that the decomposition of diphenylketone occurs at higher aging temperatures. Diphenylketone decomposes and then be oxidized to quinone, acids, or esters.[4,19] The possible reaction in soft segment of EPN is shown in Scheme 1A. The presence of diphenylketone and quinone as chromophore groups changes the material color, which coincides with the color changes of SW/EPN composites.

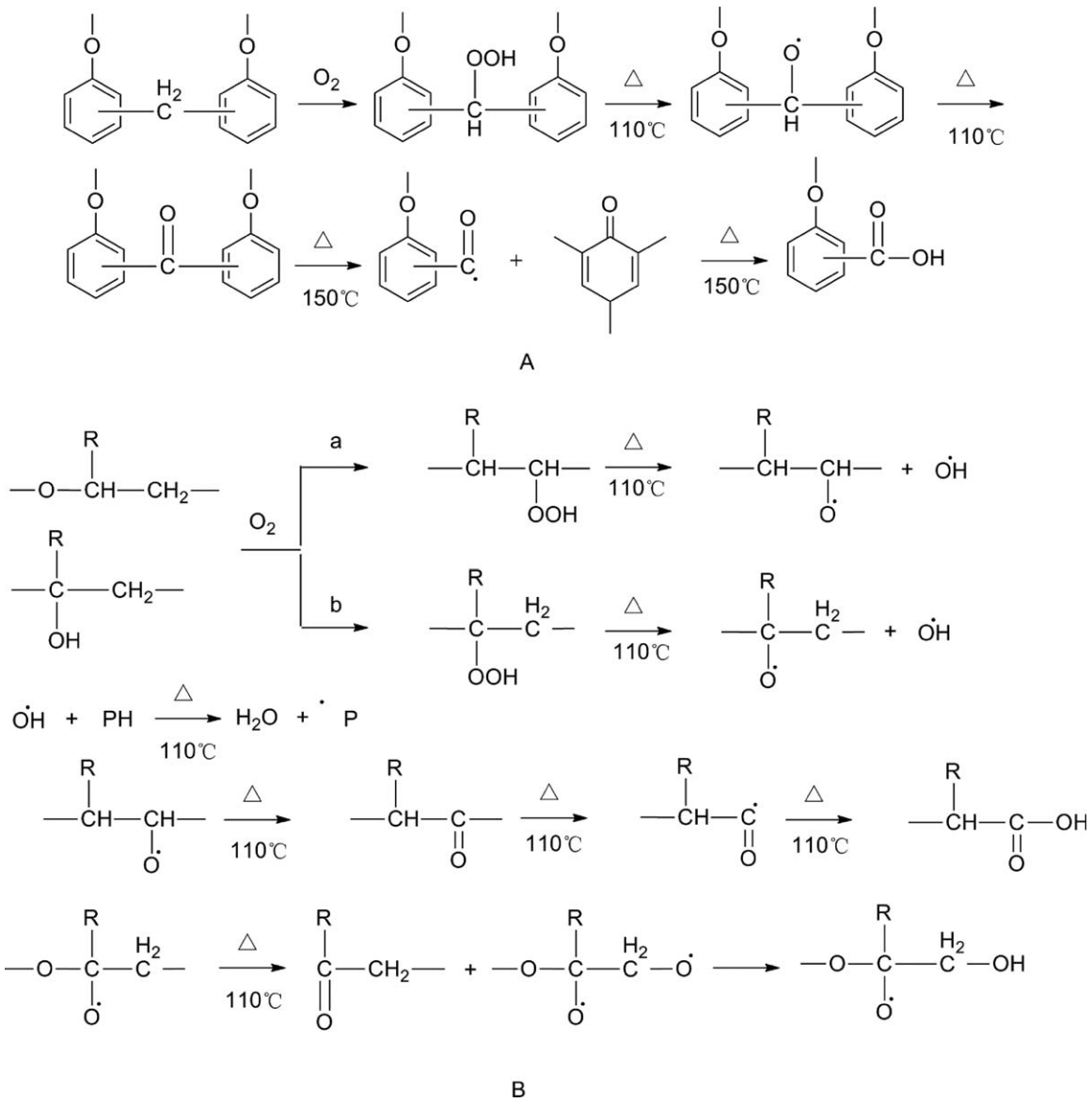

Scheme 1. Possible reactions in hard segment (A) and soft segment (B) of EPN.

In addition, the band near 1725 cm^{-1} is assigned to the C═O in acid or ester. Due to the formation of saturated acid or ester, the intensity of COOR rises with the extension of aging time as shown in Figure 7(C). When specimen aged at 150°C or 170°C, the outstanding decline of COOR during the final aging period is indicative of the decomposition of ester. Furthermore, the decrease in intensities of COOR is larger than that of C═O, which indicates that diphenylketone possesses higher thermal stability compared with acid or ester. The probable reaction in hard segment of EPN is shown in Scheme 1B.

The absorbance variation of R—O—R with aging process at four aging temperatures is shown in Figure 7(D). For specimens aged at 110°C, 130°C, and 150°C, the intensity of R—O—R increases first and then decreases with ongoing of aging time. The increase of R—O—R is attributed to the condensation between phenolic hydroxyl and hydroxyl during post curing, while its decline results from the decomposition of the forming R—O—R. When the aging temperature is 170°C, the intensity of R—O—R fluctuates slightly with aging time. It manifests that post curing improved the thermal stability of EPN.

As we all know, the polarity of substituent group affects the intensity of Ar. The intensity of Ar increases with aging process as shown in Figure 7(E). It may be attributed to the oxidation of CH_2 between two benzene rings and the formation of cross-linking network. Hence the oxidation and post curing of EPN during hot air aging can be confirmed.

The group contents of EPN were measured by XPS to verify the chemical changes of EPN. The C_{1s} spectra and corresponding group contents on the surface of EPN under various aging conditions are given in Figure 8. There are five carbon-based functional groups including C—C (graphitic carbon, 284.8 eV), C*—C═O (carbon bonded ketone, acid or ester, 285.6 eV),

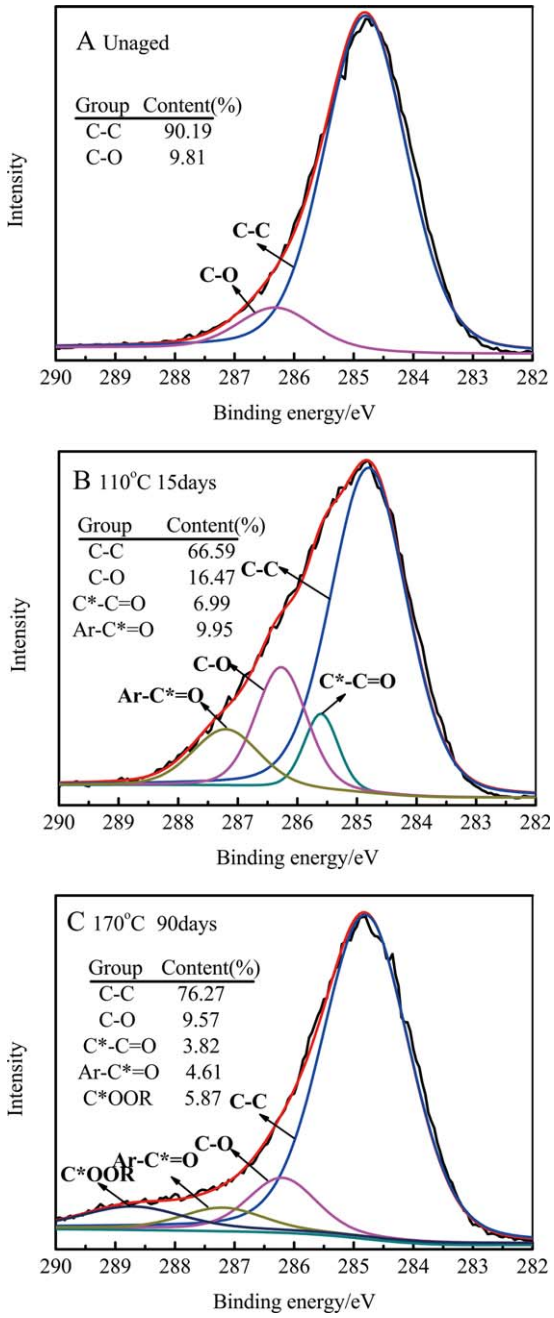

Figure 8. C_{1s} spectra of EPN for various aging conditions: (A) Unaged, (B) 110°C, 15 days, (C) 170°C, 90 days. [Color figure can be viewed in the online issue, which is available at wileyonlinelibrary.com.]

C—O (carbon bonded phenolic, alcohol hydroxyl, or ether oxygen, 286.4 eV), Ar—C*—O (carbonyl carbon bonded benzene ring, 287.2 eV), and C*OOR (carboxyl functions or ester groups, 288.8 eV).[21–23]

As shown in Figure 8(A), two bands of C—C and C—O are observed from the C_{1s} spectra of unaged EPN, and the relative contents of C—C and C—O are 90.19% and 9.81%, respectively. As can be seen from Figure 8(B), when samples aged at 110°C for 15 days, the bands of C*—C═O and Ar—C*═O appear and the content of the C—C decreases to 66.59% because CH_2 is oxidized to carbonyl. The phenomenon is consistent with the growth of C═O and COOR, in company with the decline of CH_2 [see Fig. 7(A–C)], which are obtained by FTIR. Meanwhile, the content of C—O increases to 16.47% because of the post-curing. It coincides with the increasing R—O—R in the initial aging period [see Figure 7(D)]. For the sample aged at 170°C for 90 days, the peak of C*OOR is discovered in Figure 8(C). Meanwhile, the relative contents of Ar—C*═O and C*—C═O decrease to 4.61% and 3.82%, respectively. These figures suggest that Ar—C*═O and C*—C═O are oxidized to COOR at higher aging temperatures. The XPS results also correspond to those shown in FTIR.

Changes of Thermal-Mechanical Properties of EPN

The degradation occurring during aging is accompanied by a variation in molecular mobility. These variations can be monitored by the glass temperature, T_g. Moreover, the evolution of T_g of epoxy resin is the same as its composites after thermal aging.[17] Therefore, the evolution of T_g of composites can be investigated by that of EPN. The loss factors, tan δ, measured as a function of temperature are shown in Figure 9. In addition, the evolution of the corresponding T_g of EPN with different aging time and temperatures is shown in Figure 10. The T_g is defined by the tan δ peak in this study.

As shown in Figure 9(A), for unaged EPN sample, two peaks in tan δ curves were observed. And Figure 10 shows that the two corresponding T_g are 197°C (T_{g1}) and 283°C (T_{g2}), respectively. This phenomenon may be attributed to the structure of phenolic and epoxy in EPN. Moreover, T_{g1} should be attributed to the soft segment comprised of aliphatic ether, and T_{g2} should be assigned to the hard segment consisting of the main chain of phenol. After aging at 110°C, the two peaks in tan δ curves gradually shift to the middle and become less obvious with the ongoing of aging time. That is to say, as aging time extends, T_{g1} shifts to higher temperatures while T_{g2} shifts to lower temperatures (see Figure 10).

As shown in Figure 9(B–D), when aging at 130°C, 150°C, or 170°C, the tan δ curves show the similar characteristics, and the tan δ increases with the increase of aging temperature. In addition, in the final period of aging at 150°C and 170°C, there is only one peak in tan δ curves. Meanwhile, Figure 10 shows that the changing trends of T_{g1} and T_{g2} at 130°C, 150°C, or 170°C are the same as that at 110°C. And the change in curves of T_{g1} and T_{g2} coincide with each other after aging for 60 days at 150°C or 30 days at 170°C, namely, only one T_g is observed. Hence the system is uniform due to the formation of the perfect crosslinked networks after post curing.

The T_g is related to crosslinking density, chemical structure, and molecular weight. The results of FTIR show that the crosslinking density and chemical structure of EPN are respectively affected by post curing and oxidation, and the molecular weight of EPN is affected by decomposition. The above three effects lead to the weight changes of EPN. Therefore, the changes in T_g are related to the mass loss. Because the mass loss of SW is negligible, the mass loss of the EPN can be taken as that of SW/EPN.

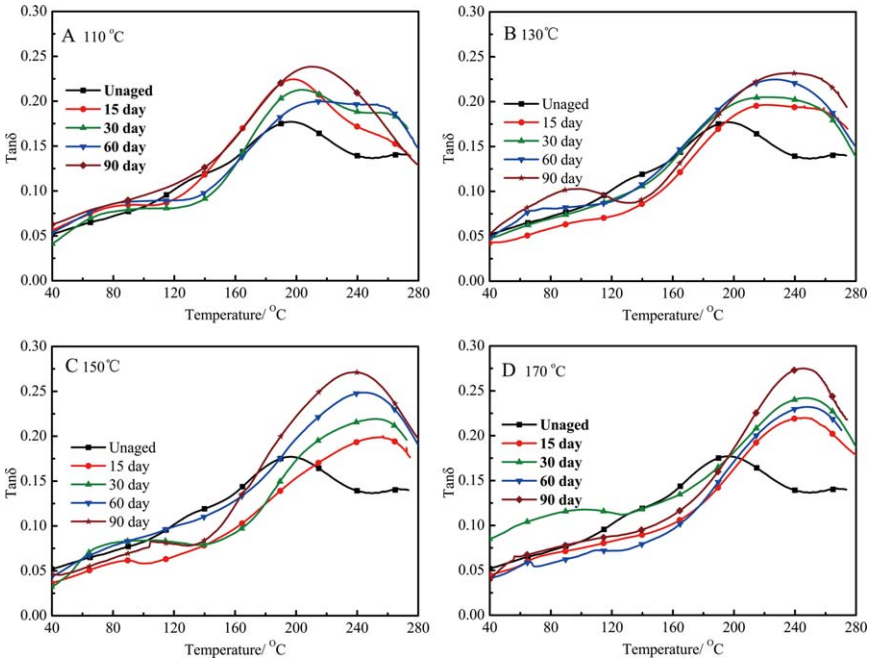

Figure 9. Curves of tan δ of EPN over aging time at different temperatures. [Color figure can be viewed in the online issue, which is available at wileyonlinelibrary.com.]

Figure 11 shows the curves of T_{g1} and T_{g2} versus the mass loss of SW/EPN. As shown in the Figure 11, T_{g1} increases while T_{g2} decreases with the increase of weight loss. In the final period of aging at 170°C, T_{g1} and T_{g2} remain constant, whereas the decomposition of EPN occurs predominantly according to the analysis of FTIR. Therefore, the thermal decomposition of EPN has little effect on the variation of T_{g1} and T_{g2}.

In order to determine the effect of post curing and oxidation on the T_g, the bands at 1610 cm^{-1} and 1650 cm^{-1} were respectively chosen. The curves of T_{g1} versus the absorbance of Ar and T_{g2} versus the absorbance of C═O are shown in Figure 12. The absorbance of Ar near 1610 cm^{-1} is related to the amount of crosslink of soft segment occurring between phenolic hydroxyl and hydroxyl. And the absorbance of C═O near 1650 cm^{-1} reflects the amount of oxidation of CH_2 between two benzene rings in hard segment.

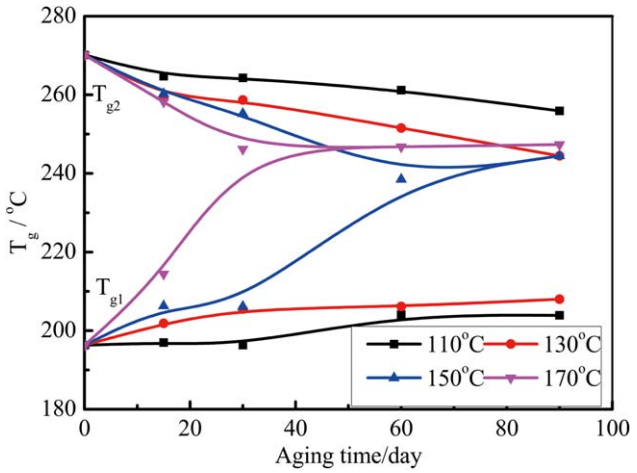

Figure 10. Curves of T_g of EPN over aging time at different temperatures. [Color figure can be viewed in the online issue, which is available at wileyonlinelibrary.com.]

The T_{g1} obtained at different temperatures is expressed as a function of the absorbance of Ar as shown in Figure 12(A). When specimens are aged at 110°C or 130°C, a positive linear relationship between T_{g1} and the absorbance of Ar can be observed. Therefore, the increase of T_{g1} is attributed to the post curing of EPN. After aging for 60 days at 150°C or for 30 days at 170°C, the T_{g1} increases rapidly and then remains relatively constant. The possible reason is the formation of perfect crosslink network. In Figure 12(B), the T_{g2} and the absorbance of C═O show a negative linear relationship, but no significant influence of the temperatures applied. These suggest that the variation of T_{g2} is assigned to the oxidation of hard segment of EPN.

CONCLUSIONS

In this article, the response behavior of microstructure evolution to thermal air aging of SW/EPN composites was investigated. The main conclusions are as follows:

1. The physical changes of SW/EPN composites were studied by color variation, mass loss, and the fiber–matrix interface evolution during hot air aging. The formation of chromophore groups leads to the color changes of SW/EPN composites from pale yellow to black. The mass loss of SW/EPN composites depends on the aging temperature and aging time. Moreover, the degradation of EPN plays a major role in that of SW/EPN composites. The volatilization of small molecules and pyrolysis products leads to cracks initiation and propagation at the fiber–matrix.

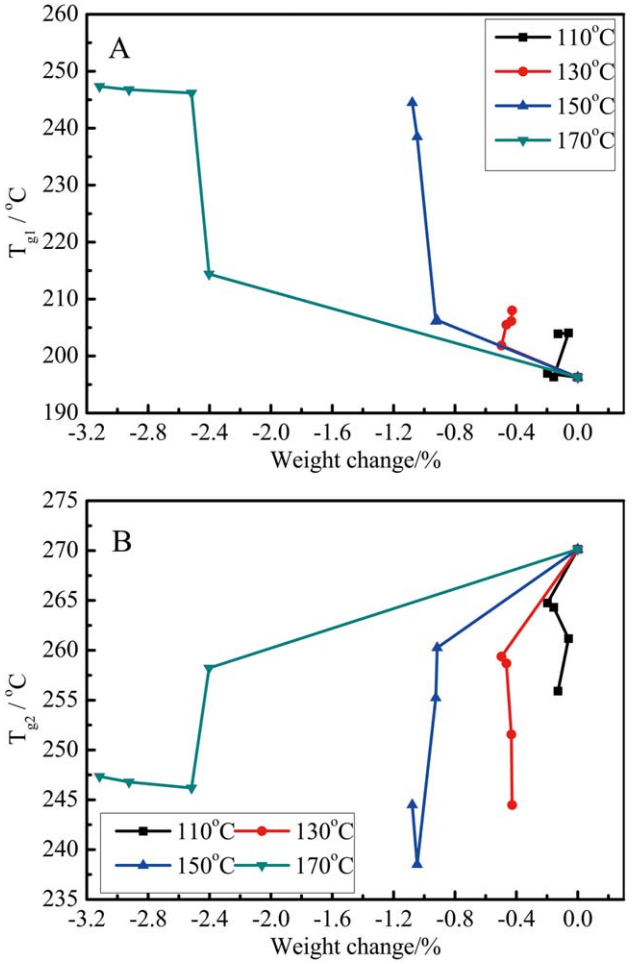

Figure 11. Curves of T_{g1} and T_{g2} of EPN versus the weight change of SW/EPN. [Color figure can be viewed in the online issue, which is available at wileyonlinelibrary.com.]

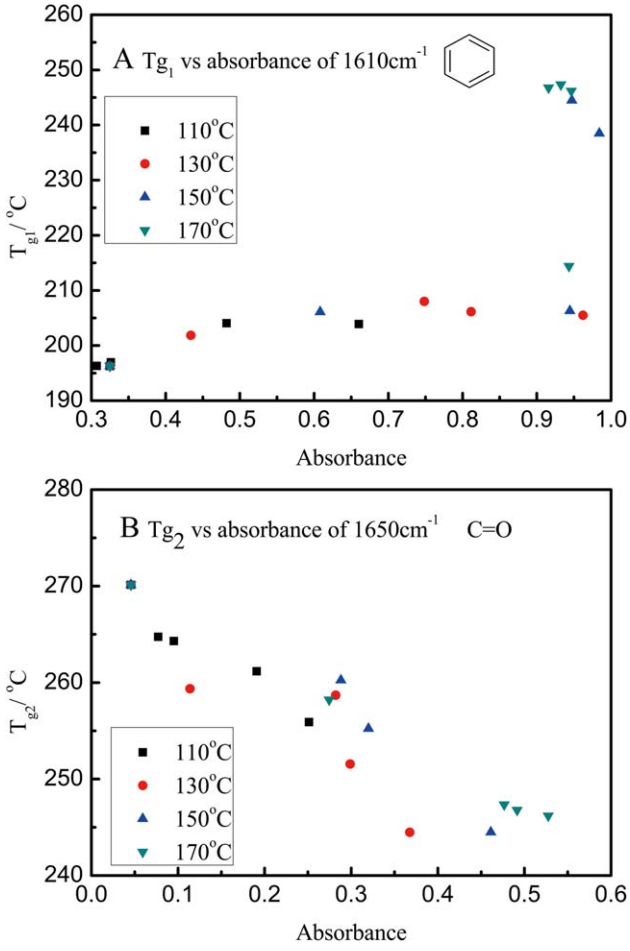

Figure 12. Curves of T_{g1} versus the absorbance of Ar and T_{g2} versus the absorbance of C=O. [Color figure can be viewed in the online issue, which is available at wileyonlinelibrary.com.]

2. The chemical changes of EPN were carried out by FTIR and XPS. The overall hot air aging process of EPN consists of post curing, oxidation, and thermal decomposition. Moreover, post curing occurs in the initial aging period. In addition, methylene in many positions is oxidized to carbonyl during the whole aging process. In the finial aging period, the formed carbonyl decomposes and then be oxidized to acids or esters at higher temperatures.
3. The evolution of T_g was monitored by DMTA, and the relationship between T_g and chemical structure, as well as T_g and mass loss was investigated. For the unaged EPN sample, two T_g are observed at 196°C (T_{g1}) and 270°C (T_{g2}), and T_{g1} and T_{g2} respectively refer to the T_g of the soft segment and the hard segment. As aging time increases, T_{g1} increases for post curing while T_{g2} decreases for oxidation. In the final period of aging at higher temperatures, only one T_g is observed due to the forming of perfect network. In addition, the thermal decomposition of EPN has little effect on the variation of T_{g1} and T_{g2}.

These results provide insightful reference value to investigate the failure mechanism and the life of SW/EPN composites in service and storage period.

REFERENCES

1. Tsotsis, T. K. *J. Compos. Mater.* **1995**, *29*, 410.
2. Lafarie-Frenot, M. C.; Rouquie, S. *Compos. Sci. Technol.* **2004**, *64*, 1725.
3. Celina, M. C.; Dayile, A. R.; Quintana, A. *Polymer* **2013**, *54*, 3290.
4. Pei, Y. M.; Wang, K.; Zhan, M. S. *Polym. Degrad. Stab.* **2011**, *96*, 1179.
5. Olivier, L.; Baudet, C.; Bertheau, D. *Compos. A* **2009**, *40*, 1008.
6. Han, J.; Kim, C. *Compos. Struct.* **2006**, *72*, 218.
7. Vu, D. Q.; Gigliotti, M.; Lafarie-Frenot, M. C. *Compos. A* **2012**, *43*, 577.
8. Bockenheimer, C.; Fata, D.; Possart, W. *J. Appl. Polym. Sci.* **2004**, *9*, 361.
9. Galant, C.; Fayolle, B.; Kuntz, M. *Prog. Org. Coat.* **2010**, *69*, 322.
10. Mailhot, B.; Morlat-Therias, S.; Ouahioune, M. *Macromol. Chem. Phys.* **2005**, *206*, 575.
11. Awaja, F.; Pigram, P. *J. Polym. Degrad. Stab.* **2009**, *94*, 651.

12. Wolfrum, J.; Eibl, S.; Lietch, L. *Compos. Sci. Technol.* **2009**, *69*, 523.
13. Colin, X.; Mavel, A.; Marais, C. *J. Compos. Mater.* **2005**, *39*, 1371.
14. Pochiraju, K. V.; Tandon, G. P.; Schoeppner, G. A. *Mech. Time-Depend. Mater.* **2008**, *12*, 45.
15. Boucher, V.; Rain, P.; Teissedre, G. IEEE-Conference on Electrical Insulation and Dielectric Phenomena, Quebec, Canada, **2008**; p 83.
16. Boucher, V.; Rain, P.; Teissedre, G. *IEEE-International Conference on Solid Dielectrics*, Winchester, UK, **2007**, p 162.
17. Leveque, D.; Schieffer, A.; Mavel, A. *Compos. Sci. Technol.* **2005**, *65*, 395.
18. Xia, Y. W.; Wo X. Y. *Spacecraft Recov Remote Sensing* **2004**, *25*, 40.
19. Guo, D. D.; Zhan, M. S.; Wang, K. *J. Appl. Polym. Sci.* **2012**, *126*, 2010.
20. Hong, S. G. *Polym. Degrad. Stab.* **1995**, *48*, 211.
21. Song, W.; Gu, A.; Liang, G. *Appl. Surf. Sci.* **2011**, *257*, 4069.
22. Chilkoti, A.; Ratner, B. D. *Surf. Interface Anal.* **1991**, *17*, 567.
23. Payne, R. S.; Beamson, G. *Polymer* **1993**, *34*, 1637.